Chinese Journal of Polymer Science Vol. 33, No. 3, (2015), 386–394

Chinese Journal of Polymer Science
© Chinese Chemical Society
Institute of Chemistry, CAS
Springer-Verlag Berlin Heidelberg 2015

Phase Structure and Crystallization Behavior of Polyethylene in Its Blends with *cis*-1,4-Butadiene Rubber*

Hong Yao, Jun-teng Liu, Li-qun Zhang and Shou-ke Yan**
Beijing Key Laboratory of Membrane Science & State Key Laboratory of Chemical Resource Engineering, Beijing University of Chemical Technology, Beijing 100029, China

Abstract Phase structure and crystallization behavior of polyethylene (PE) in its blends with *cis*-1,4-butadiene rubber (BR) at different blend ratios and sample preparation conditions were studied. The PE is finely dispersed in the BR matrix. For samples hot pressed at 145 °C, circular PE microdomains with randomly oriented PE lamellar aggregates were produced. The domain size and number increase with increasing PE content. When the PE content is over 10 wt%, most of the PE domains impinged each other. The separated PE domains are connected by PE stripes with parallel arranged lamellar aggregates. For samples hot pressed at 140 °C, elongated PE microdomains with oriented PE lamellar aggregates were obtained due to the shear flow. The crystallization of PE in the blends depends on the phase structure. Confined crystallization of PE occurs in small microdomains at relatively low temperature. With the increase of domain size, the crystallization ability of PE increases while the confined crystallization decreases.

Keywords: Polyethylene; *cis*-1,4-Butadiene rubber; Blend; Crystallization; Morphology.

INTRODUCTION

Polymer blends have received much attention for many decades since it provides an effective and simple way to obtain new materials with desired performances. There are many researches of thermoplastic resin and rubber blends including thermoplastic vulcanizates and thermoplastic elastomers, which have reached a high level of significance in the field of polymer blends[1–21]. In this kind of blends, thermoplastic resins could be toughened with rubbers to get high performance thermoplastics when the rubber is a minority component and *vice versa* the rubbers can be reinforced by thermoplastics when the rubber is a rich phase. For example, polyethylene (PE) and polypropylene are often used as rubber reinforcing agents, which offer the advantages of a better mixing, less reactor fouling, and easy recycle of the material[19, 22].

Cis-1,4-polybutadiene (BR) as one of the most important synthetic elastomers has many practical applications in tire industry and mechanical goods. It exhibits very low glass transition temperature of about −106 °C and flexible molecular chains, excellent resilience, good abrasion resistance, damping behavior and low temperature performance[23, 24]. The drawbacks of it rest on its poor wet traction, rolling resistance, tear resistance and tensile strength. Therefore, blending of it with thermoplastics, such as polystyrene, polypropylene, ethylene vinyl acetate, polycaprolactone and PE, has attracted much attention for getting materials with desired performance as well as for understanding the fundamental problems of polymer blend systems[19, 24–32]. High-density polyethylene has high tensile modulus, high crystallinity and fast crystallization rate. It was therefore ideal to improve tear resistance and tensile strength of BR. The studies about PE/BR blends are mainly focused

* This work was financially supported by the National Natural Science Foundation of China (Nos. 21274009 and 51221002).
** Corresponding author: Shou-ke Yan (闫寿科), E-mail: skyan@mail.buct.edu.cn
Received May 16, 2014; Revised September 5, 2014; Accepted September 18, 2014
doi: 10.1007/s10118-015-1592-4

on the processing parameters, interfacial adhesion, mechanical properties, and so on. It should be pointed out that the morphologies, especially the phase structure which is affected by crystallization and in turn affects the crystallization behavior of the crystalline component[33−37], show great influence on the final properties of the blend materials. The phase structure and crystallization behavior of PE/BR blends have rarely been studied. Therefore, in this work, phase structure and the crystallization behavior of PE/BR blends were studied.

EXPERIMENTAL

Cis-1,4-polybutadiene (BR, trade name BR9000, *cis*-1,4-content > 97%, M_n = 6.6 × 10^4 g/mol, M_w/M_n = 5.2, Mooney viscosity ML1+4 at 100 °C = 47) and high density polyethylene (PE, trade name HDPE7600M, a commercial bimodal PE100 resin) were obtained from Sinopec Yanshan Petrochemical Co., SINOPEC, Beijing, China. The number average molecular weight of PE is 1.0 × 10^4 and its molecular weight distribution index is 27.4.

PE/BR blends with different PE contents ranging from 0 wt% to 30 wt% were prepared in a Haake Polylab Reomixer 600P internal batch mixer connected to a controlled unit (Haake PolyLab A) at 145 °C for 10 min. The rotor rate was set at 50 r/min. Thin films for microscopy observation were prepared by hot compression mold a small amount of PE/BR blend. The hot compression mold was conducted at either 145 °C or 140 °C for 5 min and then cooled quickly down by relocating the pressed sample to another press stage at room temperature under pressure. The film thickness was estimated to be ~30 μm for all samples. Before microscopy observation, unless otherwise stated, all of the samples were further heat-treated under atmosphere pressure at a hot stage at 145 °C for 5 min to release residual thermal stress, then quickly transferred to a hot stage at 125 °C for 1 h, and finally cooled down under room temperature in air.

Optical microscopy observations were conducted on a Carl Zeiss Axioskop 40A Pol optical microscope equipped with a hot stage (Linkam THMS600/CI94). The temperature accuracy is (± 0.1) K. All pictures shown in this paper were taken under crossed polarizers.

Scanning electron microscopy (SEM) observation was performed on a JEOL JSM 6700F instrument operated at 5 kV. The specimens were sputtered with a thin layer of gold before observation.

Calorimetric studies were carried out in a Q2000 differential scanning calorimeter (TA Instruments, USA) calibrated with indium and zinc. Nitrogen was used as a purge gas. Samples of 5−10 mg were encapsulated and sealed in aluminum pans. The thermal history of the samples was erased by heating to 170 °C for 5 min. Cooling scans were registered at 10 K/min within the temperature window of −70 to 170 °C.

RESULTS AND DISCUSSION

Figure 1 shows the optical micrographs of PE/BR blends with different blend ratios. The samples were hot pressed at 145 °C. Under crossed polarizers, the BR component does not provide any birefringence due to its amorphous feature at room temperature. Therefore, the birefringence shown in Fig. 1 is solely contributed by the PE crystals. From Fig. 1, we can see that phase separation takes place in all of the blends. The PE microdomains well dispersed in the BR matrix regardless of its composition. In the separated microdomains, the PE crystallizes in microcrystallites instead of spherulities. The increase of birefringence with increasing PE content indicates an increment of the amount of PE crystals. To reveal the crystal growth process of the PE component, *in situ* optical microscopy observation was performed.

Figure 2 presents the optical micrographs of a 10/90 PE/BR blend taken during the isothermal crystallization at 125 °C. From Fig. 2(a), some sparsely dispersed bright dots with weak birefringence, reflecting the crystalline PE phases, can be seen after 40 min at 125 °C. This indicates the occurrence of PE crystallization. With time extending, the birefringence of the existing crystalline PE dots becomes brighter and brighter, while new bright dots appear gradually, indicating the proceeding of the PE crystallization. After 210 min at 125 °C, see Fig. 2(c), large quantity of PE crystalline microdomains evenly dispersed in the BR matrix have been observed. Thereafter, morphological changes can hardly be identified under optical microscope. One may

associate this phenomenon to the completion of the PE crystallization. It is actually not the case. By comparing Fig. 2(c) with Fig. 1(d), we can see that the birefringence of the sample shown in Fig. 2(c) is somewhat weaker than that shown in Fig. 1(d), where secondary crystallization of PE and perfection of PE crystals may occur after cooling the sample to room temperature. To confirm this conclusion, the sample was also cooled to room temperature after isothermally crystallized at 125 °C for 210 min. As presented in Fig. 2(d), we see remarkable enhancement of the birefringence. This demonstrates the existence of supercooled PE melt after 210 min isothermal crystallization at 125 °C, which crystallizes *via* further cooling of the sample. From this result, it is concluded that the crystallization ability of PE in the blend is suppressed to some extent considering the bulk crystallization of PE at 125 °C finishes generally within 1 h. This should be attributed to the confined crystallization of PE in the separated microdomains[38].

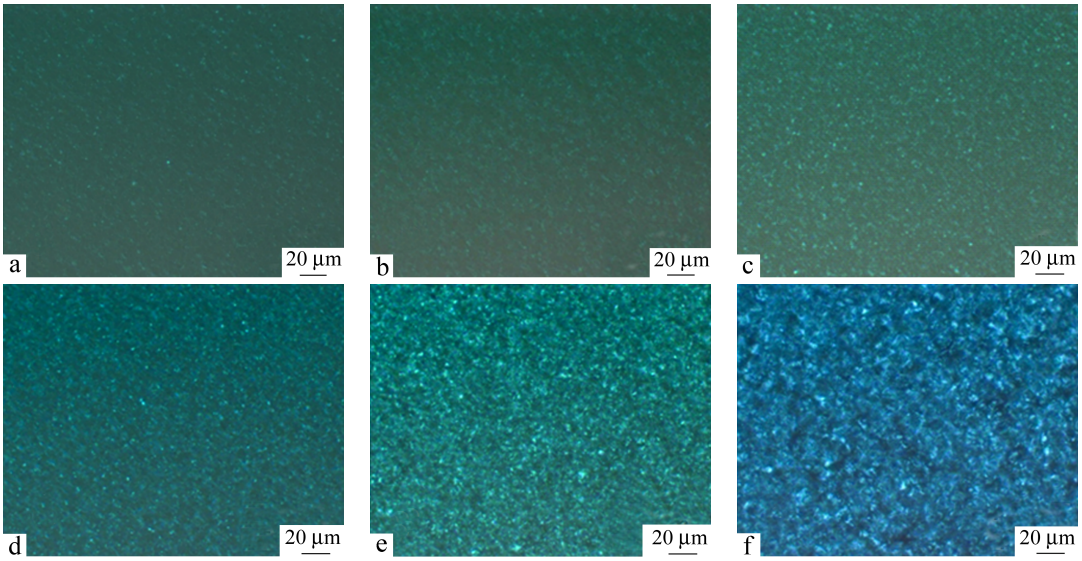


Fig. 1 Optical micrographs of PE/BR blends with different blend ratios hot pressed at 145 °C and cooled directly to room temperature in air (a) 3/97, (b) 5/95, (c) 7/93, (d) 10/90, (e) 20/80 and (f) 30/70

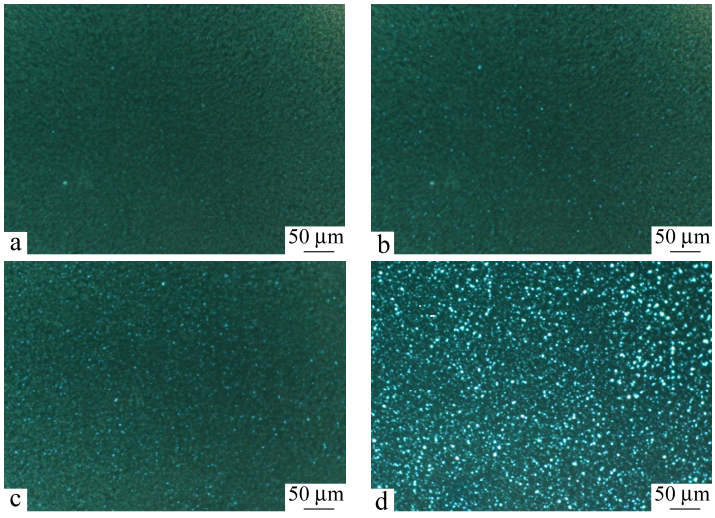


Fig. 2 Optical micrographs of a 10/90 PE/BR blend hot pressed at 145 °C taken during isothermal crystallization at 125 °C for (a) 40 min, (b) 80 min, (c) 210 min and (d) cooled to room temperature in air

DSC experimental results support the above ratiocination. Figure 3 shows the DSC cooling scans of the PE/BR blends with different blend ratios. The characteristic data including crystallization peak temperature (T_c), crystallization enthalpy (ΔH_c) and crystallinity (X_c) obtained from the DSC experiments are listed in Table 1. In Fig. 3, totally three exothermic peaks have been observed in all of the DSC cooling curves. While the exothermic peaks located at higher temperatures (around 115 °C) correspond to the crystallization of PE and therefore referred as $T_{C1,PE}$ in Table 1, the ones appeared at very low temperatures (about −30 °C) reflect the crystallization of BR matrix and indicated as $T_{C,BR}$. Another tiny exothermic peak near 80 °C is also assigned to the crystallization of PE ($T_{C2,PE}$) since crystallization of BR at this temperature is not possible. This confirms the occurrence of fractionated crystallization of PE in the blend with some of it crystallizes at higher temperature whereas the remaining part crystallizes at lower temperature. It is recognized that the exothermic peak of the early crystallized PE shifts somewhat to higher temperature. Moreover, the higher peaks become narrow and sharp with increasing PE content. This indicates that the crystallization ability of PE in the blend increases with increasing content. On the other hand, the lower crystallization temperature remains almost unchanged at ~80 °C, indicating a similar confined crystallization mechanism of the PE in small microdomains.

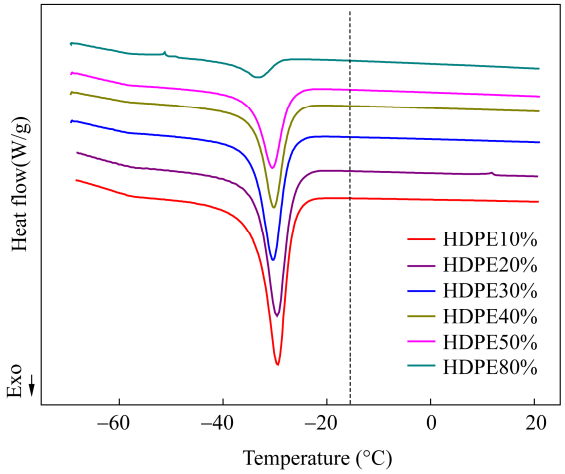


Fig. 3 DSC cooling curves of PE/BR blends with variant compositions as indicated (The cooling rate is 10 K/min.)

Table 1. The characteristic data of PE/BR blends obtained from DSC experiments

Sample	5/95 PE/BR	10/90 PE/BR	20/80 PE/BR	30/70 PE/BR
$T_{C1,PE}$ (°C)	112.02	113.96	116.29	116.92
$\Delta H_{C1,PE}$ (J/g)	4.65	13.56	29.29	43.94
$X_{C1,PE}$ (%)	32.0	46.7	50.5	50.5
$T_{C2,PE}$ (°C)	81.86	81.60	81.23	80.57
$\Delta H_{C2,PE}$ (J/g)	2.22	1.03	0.94	0.86
$X_{C2,PE}$ (%)	15.3	3.6	1.6	1.0
Overall X_{PE} (%)	47.3	50.3	52.1	51.5
$T_{C,BR}$ (°C)	−29.67	−29.40	−29.54	−30.36
ΔH_{BR} (J/g)	39.05	36.60	31.31	25.22
ΔH_{BR}^* (J/g)	41.11	40.67	39.14	36.03

Notes: ΔHBR^* is the corrected crystallization enthalpy per unit BR mass in the blends. The fusion enthalpy of the perfectly crystallized PE adopted for crystallinity calculation, *i.e.* ΔH_f^0, is selected from literature as 293 J/g[39].

From Table 1, it is clear that the output of heat during high temperature crystallization of PE, *i.e.* the $\Delta H_{C1,PE}$, increases with increasing content of PE, indicating an increased amount of PE crystals produced at high temperature. The $\Delta H_{C1,PE}$ value of the PE/BR 30/70 blend is approximately 10 times higher than that of the PE/BR 5/95 blend. Considering that the PE amount in the 30/70 blend is only 6 times as that in the 5/95 blend,

the increment of $\Delta H_{C1,PE}$ is not simply attribute to the increase of PE content but also an enhanced crystallization ability of PE. It can be seen from Table 1 that the crystallinity of PE achieved during the high temperature crystallization increases first with increasing PE content and then remains unchanged. The highest crystallinity reaches approximately 50%. On the other hand, the output of heat during low temperature crystallization of PE, *i.e.* the $\Delta H_{C2,PE}$ in Table 1, decreases slightly with increasing PE content, indicating the amount of PE crystals produced *via* confined crystallization decreases a little bit with increment of PE in the blends. This demonstrates that the confined PE melt in each blend system is more or less about the same. It should be pointed out that the PE in the blends, except for the 5/95 one, exhibits actually a similar overall crystallinity (see Table 1). This can be understood in the following way. At lower PE load, *e.g.* in the 5/95 blend, the finely dispersed PE in the BR matrix exists generally in small microdomains. This leads to the crystallization of relatively a higher proportion of PE in a confined environment. As a result, the crystallization of PE at high temperature is severely suppressed, leading to a much lower $X_{C1,PE}$ value. However, the confined crystallization of PE during further cooling of the sample is more evident than other samples. For the 10/90 PE/BR sample, the size of most PE microdomains increases. This results in the crystallization of PE in most domains takes place at high temperature, even though some PE in quite small microdomains still crystallizes during further cooling, and therefore enhances the crystallization ability of PE at high temperature. Taking into account that only small amount of PE crystallized in the confined space, the crystallinity of PE is mainly controlled by the crystallization in the first step at high temperature. Consequently, the overall crystallinity of PE in the blend increases remarkably compared to the 5/95 blend. With further increase of the PE content, even larger PE domains do not change the crystallization behavior of PE in large microdomains anymore. This causes a similar overall crystallinity of PE in all blends with more than 10 wt% PE.

The BR crystallizes in all blends at approximately –30 °C. This demonstrates that the addition of PE does not influence the crystallization temperature of BR. It is reasonable since the BR in all blends exists as a continuous matrix and no confined crystallization of BR occurs. Moreover, the similar crystallization behavior of BR in all blends also indicates that the PE exhibits no nucleation ability towards BR. It should be pointed out that the ΔH_{BR} value decreases gradually with the increase of PE content. The decrease of ΔH_{BR} value indicates a reduction of the amount of BR crystals. It can, however, not reflect the change of BR crystallinity directly owing to the different BR amount in each individual blend. To compare the crystallinity of BR in different blends, the crystallization enthalpy per unit BR mass was corrected by dividing the crystallization enthalpy of BR with its fraction. The obtained data are shown in the bottom line of Table 1 as ΔH_{BR}^{*}. These data reveal clearly a decrease of BR crystallinity with increasing PE content. This may indicate that some of the BR molecules are embedded in the PE microdomains. These molecular chains are excluded into the interlamellar amorphous regions of PE and lose their crystallization ability.

The above optical microscopy and DSC results indicate the existence of confined crystallization of PE embedded in BR matrix. To reveal the fine structures of the blends, SEM observations were carried out. Figure 4 shows the SEM micrographs of PE/BR blends with different blend ratios as shown in Fig. 1. It can be seen from Fig. 4, at lower PE compositions, *e.g.* less than 10 wt%, the SEM images indeed show more or less circular microdomains of PE dispersed in the BR matrix, see Figs. 4(a)–4(d). The number and size of the microdomains increase with increasing PE content. The domain size ranges from hundreds of nanometer to micrometers. In the separated microdomains, lamellar stacks of PE are clearly observed. The crystalline lamellar aggregates of PE are randomly oriented. When the PE content is over 10 wt%, with the increase of domain size and number, some of the PE microdomains impinged each other. Furthermore, the separated PE microdomains are mostly connected by PE stripes as indicated by the arrows in Figs. 4(e) and 4(f). It should be pointed out that the crystalline lamellar aggregates of PE within the big domains are somewhat wider in lateral direction. These lamellar aggregates should correspond to the crystallization of PE at high temperatures. With careful inspection, it seems that the PE crystalline lamellae in the stripes are thinner and shorter than those included in the bigger microdomains. They should be generated during the crystallization at relatively lower temperature, *i.e.* at 80 °C.

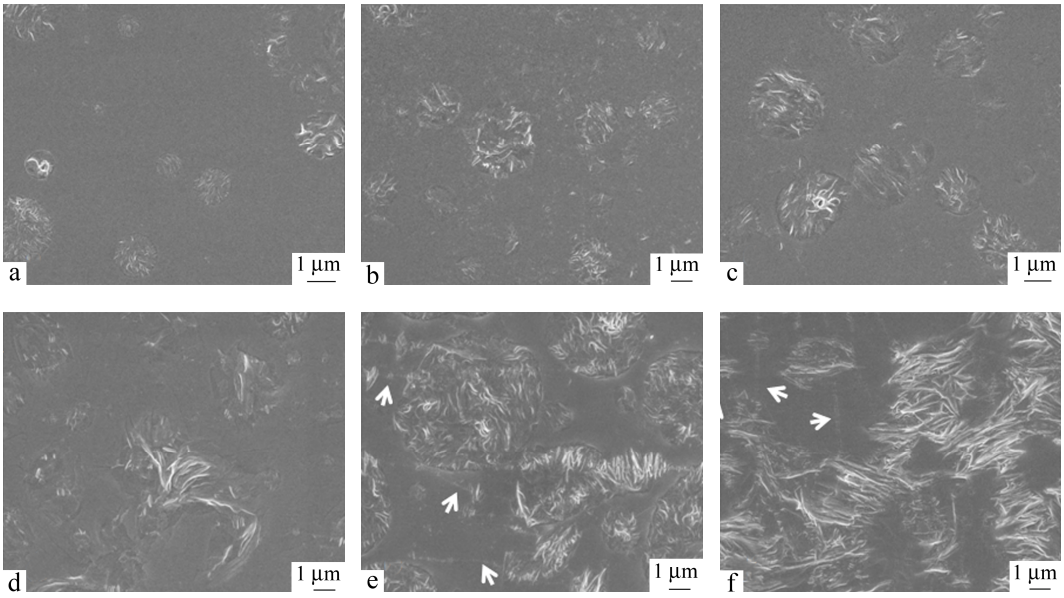


Fig. 4 SEM images of PE/BR blends of different blend ratios (a) 3/97, (b) 5/95, (c) 7/93, (d) 10/90, (e) 20/80 and (f) 30/70 hot pressed at 145 °C

It was found that the initial thin film hot press condition exhibits great influence on the phase structure of the blends and the lamellar orientation of the PE. Figures 5(a) and 5(b) shows the optical micrographs of a 30/70 PE/BR blend, which was prepared by hot compression at 140 °C for 5 min and then cooled down to room temperature under pressure. The subsequent thermal treatment after hot compression is the same as the sample shown in Fig. 1. From Fig. 5(a), we can see that the birefringence contributed by the PE crystals is more evenly dispersed in the BR matrix compared to that shown in Fig. 1(f), indicating a better distribution of PE crystals in the BR matrix. Moreover, it looks like that the PE crystals exhibit a preferred orientation in the direction from upper left to lower right. The occurrence of light extinction during rotation of the sample about the light beam axis confirms the existence of orientation[40]. As shown in Fig. 5(b), a 45° rotation of the sample around beam axis results in an evident light extinction with only weak birefringent microdots sparsely dispersed in the BR matrix. This implies that most of the PE crystals are well oriented. The oriented lamellar alignment of PE is more clearly disclosed in SEM images as shown in Figs. 5(c) and 5(d). Now lathlike microdomains of PE with width of ~1 μm and length of tens micrometers are observed in the blend. At lower magnification, see Fig. 5(c), the peculiar morphology of PE looks like the classical shish-kebab structures formed in the elongated or sheared PE melt[41, 42]. The electron micrograph with high magnification, see Fig. 5(d), reveals that the lathlike PE microdomains are composed of lamellar aggregates parallel aligned perpendicularly to the long axis of the separated PE phase. Similar oriented lamellar structure of neat PE under the same preparation condition indicates that the oriented PE lamellar structure is not related to the existence of BR. Now the elongated phase structure of PE instead of the circular PE microdomains in the matrix demonstrates the existence of flow during hot compression. Taking this into account, the oriented lamellar structures of PE should be originated from the shear flow generated during the hot press. This is acceptable under the consideration that PE has an equilibrium melting point of about 140 °C[43]. During the hot press at 140 °C, shear flow will be created when the PE melt expands outward. This leads to the orientation of PE molecular chains in flow direction. By quickly cooling the sample to room temperature under pressure, the relaxation of the oriented PE chains is suppressed. As a result, the oriented molecular chains in the melt encourage the oriented crystallization of PE, resulting in the parallel aligned lamellar structure of PE. During the subsequent thermal treatment, even though the sample was heated to 145 °C for 5 min once again, the relaxation of the molecular chains previously included in a crystal lattice is

limited. Consequently, some local order of the molecular chains previously included in a crystal lattice is preserved. These ordered molecular chains will transform into crystalline self-nuclei during cooling and trigger the oriented recrystallization of the PE again. This has been further confirmed by the crystallization behavior of PE melted at elevated temperatures.

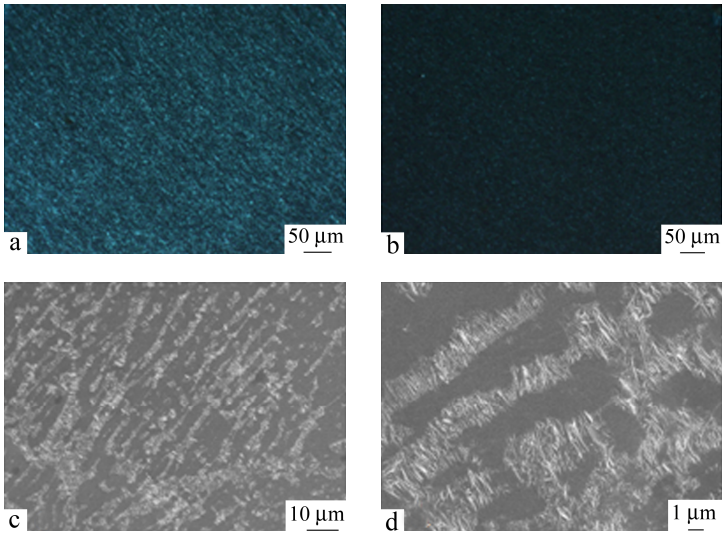


Fig. 5 Polarized optical (a and b) and SEM (c and d) micrographs of a 30/70 PE/BR blend
The thin film of the blend was pressed at 140 °C for 5 min and cooled to room temperature under pressure. After the hot compression, the sample has subjected the following heat-treatments before optical microscopy observation: heated to 145 °C for 5 min, cooled to and isothermally crystallized at 125 °C for 1 h, and finally cooled to room temperature. The part (b) is taken from the same area of part (a) but rotated for 45° about the light beam axis.

Figure 6 shows the SEM micrographs of a 30/70 PE/BR blend. The original thin film of the blend was pressed at 140 °C for 5 min and cooled to room temperature under pressure. After the hot compression, the sample was re-heated to 170 °C for 5 min, then cooled to and isothermally crystallized at 125 °C for 1 h, and finally cooled to room temperature in air. It can be clearly seen from Fig. 6 that the PE phase changed from elongated laths into circular microdomains after melting at 170 °C for 5 min. Also the molecular chains of PE relaxed completely, leading to the formation of the randomly oriented lamellar structure of PE after melt recrystallization.

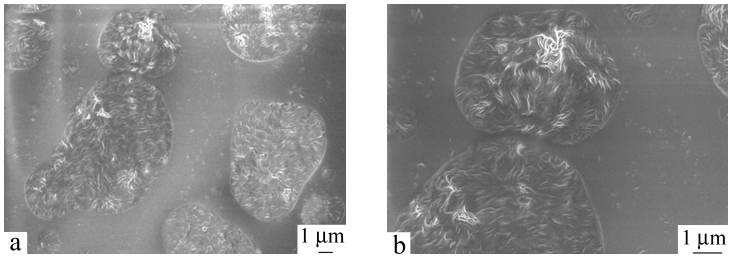


Fig. 6 SEM micrographs of a 30/70 PE/BR blend hot pressed at 140 °C for 5 min
(The sample was re-heated to 170 °C for 5 min and crystallized at 125 °C for 1 h.)

CONCLUSIONS

PE/BR blends with different blend ratios were prepared. The phase structure and crystallization behavior of PE in the blends were studied. It was found that both the phase structure and the crystalline morphology of PE are

composition and sample preparation dependent.

For the samples hot pressed at 145 °C, after further heat-treated at 145 °C for 5 min and recrystallized at 125 °C, round shaped PE microdomains were created. These microdomains were separately dispersed in the BR matrix at lower PE contents, *e.g.* less than 10 wt%. The number and size of the PE microdomains increase with increasing PE content. When the PE content is over 10 wt%, some of the PE domains impinge and fuse together, while the separated PE microdomains are connected by the PE stripes. In the microdomains, randomly oriented lamellar aggregates are observed. The strips connecting the separated domains are, however, composed of parallel aligned lamellar aggregates.

For the samples hot pressed at 140 °C, after the same further heat-treatment, elongated PE microdomains were created. In the elongated PE domains, oriented lamellar crystals of PE aligned perpendicular to the long axes of the microdomains were observed. It is confirmed that the oriented crystallization of PE is solely a result of flow-induced crystallization of PE during sample preparation.

DSC results demonstrate that the PE in bigger domains shows normal crystallization at higher temperature. The PE inlaid in quite small microdomains exhibits confined crystallization at low temperatures.

REFERENCES

1 Li, Y.J., Oono, Y., Kadowaki, Y.J., Inoue, T., Nakayam, K. and Shimizu, H., Macromolecules, 2006, 39: 4195
2 Joseph, A., Koch, T., Seidler, S., Thomas, S. and Joseph, K., J. Appl. Polym. Sci., 2008, 109: 1714
3 Machado, A.V. and van Duin, M., Polymer, 2005, 46: 6575
4 López-Manchado, M.A., Kenny, J.M., Quijada, R. and Yazdani-Pedram, M., Macromol. Chem. Phys., 2001, 202: 1909
5 Litvinov, V.M., Macromolecules, 2006, 39: 8727
6 Alfarraj, A. and Nauman, E.B., Polymer, 2004, 45: 8435
7 Calvao, P.S., Chenal, J.M., Gauthier, C., Demarquette, N.R., Santos, A.M.D. and Cavaille, J.Y., Polym. Int., 2010, 59: 851
8 Saleesung, T., Saeoui, P. and Sirisinha, C., Polym. Test., 2010, 29: 977
9 Yoo, Y., Cui L., Yoon, P.J. and Paul, D.R., Macromolecules, 2010, 43: 615
10 Pichaiyut, S., Nakason, C., Kaesaman, A. and Kiatkamjornwong, S., Polym. Test., 2008, 27: 566
11 Lim, S.W., Lee, K.H. and Lee, C.H., Polymer, 1999, 40: 2837
12 Lu, K., van Duin, M., Loos, J. and de With, G., Polymer, 2012, 53: 4171
13 Ghosh, P., Chattopadhyay, B. and Kumar Sen, A., Polymer, 1994, 18: 3958
14 l'Abee, R., Sablong, R., Goossens, H., van Duin, M., Spoelstra, A. and Duchateau, R., Macromol. Chem. Phys., 2010, 211: 334
15 Larocca, N.M., Hage Jr., E. and Pessan, L.A., Polymer, 2004, 45: 5265
16 Bartczak, Z., Argon, A.S., Cohen, R.E. and Weinberg, M., Polymer, 1999, 40: 2331
17 Cigana, P. and Favis, B.D., Macromolecules, 1997, 30: 4163
18 Polizu, S., Favis, B. and Vu-Khanh, T., Macromolecules, 1999, 32: 3448
19 Maiti, M., Jasra, R.V., Kusum, S.K. and Chaki, T.K., Ind. Eng. Chem. Res., 2012, 51: 10607
20 Zou, Z.M., Sun, Z.Y and An, L.J., Chinese J. Polym. Sci., 2014, 32(3): 255
21 Guo, K.R., Xiang, S.Y., Sun, J.B. and Meng, C.G., Chinese J. Polym. Sci., 2014, 32(3): 315
22 Buonerba, A., Cuomo, C., Speranza, V. and Grassi, A., Macromolecules, 2010, 43: 367
23 Poshyachinda, S., Edwards, H.G.M. and Johnson, A.F., Polymer, 1996, 23: 5171
24 Joseph, S., Oommen, Z. and Thomas, S., Mater. Lett., 2002, 53: 268
25 Cavanaugh, T.J., Buttle, K., Turner, J.N. and Nauman, E.B., Polymer, 1998, 18: 4191
26 Sun, H., Gong, C.H., Sun, X.H. and Sheng, J., J. Macromol. Sci.; Part B Phys., 2006, 45: 821
27 Gong, X.L., Fan, Y.C., Xuan, S.H., Xu, Y.G. and Peng, C., Ind. Eng. Chem. Res., 2012, 51: 6395
28 Cho, U.R., Korea Polym. J., 1999, 3: 196

29 Cho, U.R., Korea Polym. J., 2000, 2: 66
30 Guerrault, X., Rousseau, B. and Farago, J., J. Chem. Phys., 2004, 13: 6538
31 Salomons, G.J., Singh, M.A., Bardouille, T. and Foran, W.A., Macromolecules, 1999, 32: 1264
32 Srilathakutty, R., Joseph, R. and George, K.E., J. Appl. Polym. Sci., 2000, 3: 277
33 Yang, T., Sun, X., Ren, Z., Li, H. and Yan, S., Chinese J. Polym. Sci., 2014, 32(9): 1119
34 Wang, G. and Qiu, Z., Chinese J. Polym. Sci., 2014, 32(9): 1139
35 Li, L., Liu, J., Ren, Z. and Yan, S., Chinese J. Polym. Sci., 2014, 32(9): 1199
36 Lin, D., Zhong, Z., Tang, Y., Gao, Y., He, Y., Guo, B. and Xu, J., Chinese J. Polym. Sci., 2014, 32(9): 1234
37 Zhang, L., Shi, W., Han, C.C. and Cheng, H., Chinese J. Polym. Sci., 2014, 32(9): 1260
38 Chen, N., Huang, X.C. and Xie, X.M., Acta Polymerica Sinica (in Chinese), 2013, (10): 1341
39 Li, S., Myers, S.B. and Register, R.A., Macromolecules, 2011, 44: 8835
40 Yan, C., Guo, L., Chang, H. and Yan, S., Chinese J. Polym. Sci., 2013, 32(8): 1173
41 Somani, R.H., Yang, L., Zhu, L. and Hsiao, B.S., Polymer, 2005, 46: 8587
42 Yang, J.H., Wang, C.Y., Wang, K., Zhang, Q., Chen, F., Du, R.N. and Fu, Q., Macromolecules, 2009, 42: 7016
43 Qiu, W.L., Sworen, J., Pyda, M., Pyda, E.N., Habenschuss, A., Wagener, K.B. and Wunderlich, B., Macromolecules, 2006, 39: 204